Chemical Engineering Journal 165 (2010) 265–272

Contents lists available at ScienceDirect

Chemical Engineering Journal

journal homepage: www.elsevier.com/locate/cej

Molecular sieving effect of a novel hyper-cross-linked resin

Jianhan Huang*

School of Chemistry and Chemical Engineering, Central South University, Changsha 410083, China

ARTICLE INFO

Article history:
Received 7 July 2010
Received in revised form
17 September 2010
Accepted 20 September 2010

Keywords:
Hyper-cross-linked
Resin
Adsorption
Separation
Molecular sieving effect

ABSTRACT

Chemical modification of gel-type chloromethylated polystyrene (PS) was performed and the obtained resin HJ-C01 was employed as a polymeric adsorbent for adsorptive removal of *p*-nitroaniline and separation of *p*-nitroaniline from methyl orange (or Congo red). The results indicated that micro/mesoporous structure played a predominant role in the pore diameter distribution and the average pore diameter of HJ-C01 was 2.39 nm. The adsorption of *p*-nitroaniline onto HJ-C01 from aqueous solution was effective and the adsorption capacity of *p*-nitroaniline was much larger than methyl orange and nearly no Congo red was adsorbed onto HJ-C01. Fixed-bed column adsorption experiments demonstrated that HJ-C01 was an excellent polymeric adsorbent for adsorptive removal of *p*-nitroaniline from aqueous solution and it could separate *p*-nitroaniline effectively from methyl orange (or Congo red) by molecular sieving effect.

1. Introduction

In the last two decades, there is an increasing concern for the public health and environmental pollution around the world, and water pollution caused by organic compounds has attracted many attentions. Many methods and techniques like chemical oxidation, biological degradation, member separation, solvent extraction and adsorption are developed for efficient removal of organic compounds from wastewater [1–4]. Among these methods and techniques, adsorption is proved to be efficient because it is relatively easy to operate and the organic compounds in the wastewater can be feasibly recycled [5].

Many typical adsorbents like activated carbon and clay are often applied in the adsorption for removal of organic compounds from wastewater. Activated carbon possesses high BET specific surface area and predominant micropores which are very advantageous for the adsorption. However, the relatively poor mechanical strength and poor regeneration property of activated carbon limit its field application [6]. Recently, synthetic polymeric adsorbents have shown their advantages in the aspects of mechanical strength, diverse structures and quick regeneration, and hence they are considered to be the significant alternatives to activated carbon for adsorptive removal of organic compounds from aqueous solution [7–9].

In recent years, Davankov and co-workers synthesized a novel hyper-cross-linked polystyrene (PS) resin by adding bi-functional cross-linking agents and Friedel–Crafts catalysts in Friedel–Crafts reaction [10,11]. A number of rigid methylene cross-linked bridges are formed between the polymeric chains and the polymeric skeleton is greatly reinforced accordingly. The results indicated that the obtained hyper-cross-linked PS resin has a high BET specific surface area, narrow pore diameter distribution and predominant micropores/mesopores, and hence it exhibits excellent adsorption behaviors for non-polar or weakly polar aromatic organic compounds like benzene, toluene and xylene [12,13]. Gel-type low cross-linked chloromethylated PS is a non-porous structure in dry state while it can be adequately swollen in organic solvents like nitrobenzene and 1,2-dichloroethane, and hence Friedel–Crafts reaction can also take place for gel-type low cross-linked chloromethylated PS itself [14]. In particular, the Friedel–Crafts reaction will produce a large number of micropores and a high BET specific surface area for the obtained hyper-cross-linked resin [15,16], which not only endow it with effective adsorption of aromatic organic compounds, but also making it possible for separation of aromatic organic compounds with different molecular size by molecular sieving effect [17].

In this study, a novel polymeric adsorbent HJ-C01 was synthesized from gel-type chloromethylated PS, its pore structure and surface chemical structure were characterized. HJ-C01 was then employed as a polymeric adsorbent for adsorptive removal of *p*-nitroaniline from aqueous solution. Methyl orange and Congo red were selected as the model molecules to elucidate the molecular sieving effect of HJ-C01 and the separation property of HJ-C01 for *p*-nitroaniline from methyl orange (or Congo red) was conducted.

* Corresponding author. Tel.: +86 731 88879616; fax: +86 731 88879616.
E-mail address: xiaomeijiangou@yahoo.com.cn.

1385-8947/$ – see front matter © 2010 Elsevier B.V. All rights reserved.
doi:10.1016/j.cej.2010.09.028

2. Experimental methods

2.1. Materials

Gel-type chloromethylated PS was purchased from Nankai University Chemical Plant (Tianjin, China), its cross-linking degree was 1%, chlorine content was 4.7 mmol/g and particle size was 70–90 meshes. Zinc chloride was dehydrated on an electric cooker and was deposited in a vacuum desiccator before use. *p*-Nitroaniline, methyl orange and Congo red applied as the adsorbates were analytical reagents and used without further purification, their main properties including molecular structure, molecular weight and molecular size were listed in Table 1. The molecular size was obtained from the optimized molecular structure performed by Gaussian 03 software package [18]. Hartree–Fock method with 6-31 G basis set was employed and the optimized molecular structure was achieved if there was no imaginary frequency. Their optimized molecular structure models by Gaussian View program were displayed in Fig. 1.

2.2. Synthesis and pretreatment of HJ-C01 resin

As shown in Scheme 1, 40 g of gel-type chloromethylated PS was swollen by 200 ml of nitrobenzene overnight at room temperature. At a moderate stirring speed, the reaction mixture was heated to 323 K, 2.0 g of anhydrous zinc chloride was added into the reaction mixture as soon as possible. When zinc chloride was completely dissolved, the reaction mixture was slowly and evenly heated to 388 K within 1 h, and HJ-C01 was obtained after keeping the reaction mixture at 388 K for about 10 h.

To remove the residual nitrobenzene and zinc chloride from the pores of the solid particles, the solid particles were filtrated and subjected to rinsing in turn by 1% of hydrochloric acid aqueous solution and anhydrous ethanol until the effluents from the 1% of hydrochloric acid aqueous solution were transparent. After that, the HJ-C01 was washed by de-ionized water until neutral pH, extracted by anhydrous ethanol for about 10 h and then dried in vacuum at 333 K for about 8 h.

2.3. Characterization of HJ-C01 resin

The BET specific surface area and pore diameter distribution were determined via the N_2 adsorption–desorption curves with the temperature at 77 K using a Micromeritics Tristar 3000 surface area and porosity analyzer (Micromeritics, USA). The Fourier-transformed infrared ray (FT-IR) spectra of the resin with

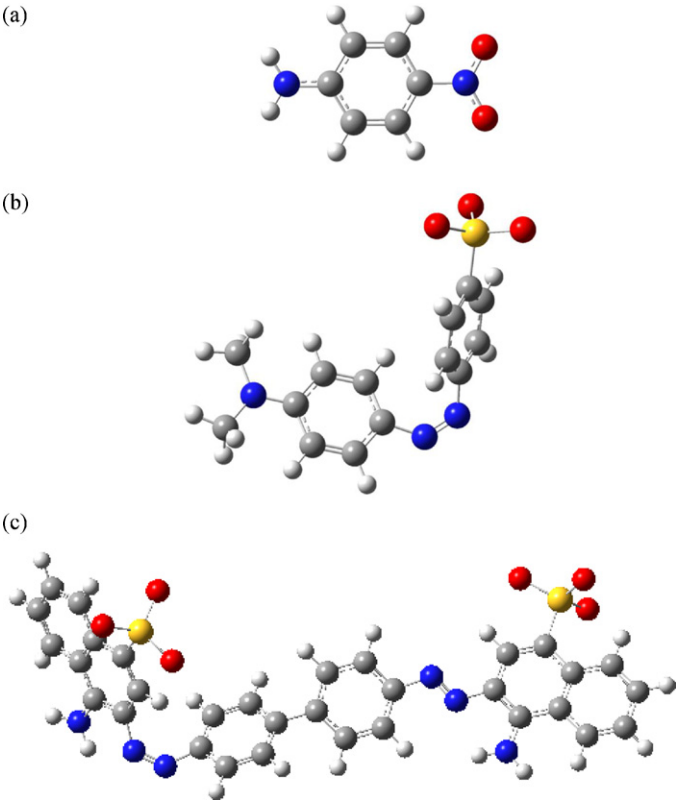

Fig. 1. The optimized molecular structure models of (a) *p*-nitroaniline, (b) methyl orange and (c) Congo red on Gaussian View program calculated by Gaussian 03 software package (Gaussian 03 program was applied for the calculation, Hartree–Fock method with 6-31 G basis set was used, the optimized molecular structure models were displayed by Gaussian View program).

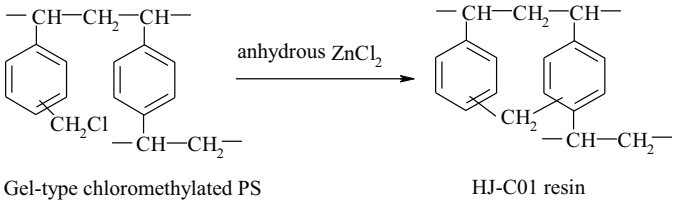

Scheme 1.

Table 1
The main properties of *p*-nitroaniline, methyl orange and Congo red.

Substance	Formula	Molecular structure	Molecular weight	Molecular size
p-Nitroaniline	$C_6H_6N_2O_2$	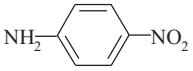	138.1	0.67 nm × 0.43 nm
Methyl orange	$C_{14}H_{14}N_3O_3SNa$	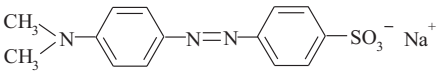	327.3	1.19 nm × 0.68 nm × 0.37 nm
Congo red	$C_{32}H_{22}N_6O_6S_2Na_2$	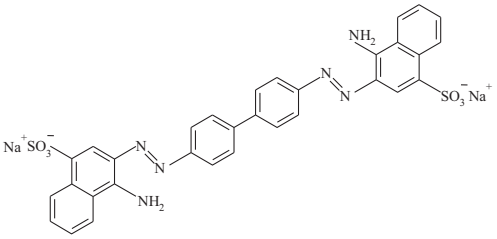	696.7	2.29 nm × 0.82 nm × 0.60 nm

Table 2
The main properties of HJ-C01 resin.

BET specific surface area (m^2/g)	Average pore diameter (nm)	Pore volume (cm^3/g)	Chlorine content (%)	Oxygen content (%)
1546.9	2.39	0.9257	4.2	3.3

vibtrational frequencies in the range of 500–4000 cm^{-1} were collected by KBr disks on a Nicolet 510P Fourier transformed infrared instrument (Nicolet, USA). The elemental analysis of the resin was obtained with a Vario EL III Elementar Analysensysteme (Elementar, Germany) and the oxygen content was calculated by the following equation:

$$O\% = 100\% - C\% - H\% - C1\% \quad (1)$$

where the residual chlorine content was performed according to Volhard method in Ref. [19]. The concentration of *p*-nitroaniline, methyl orange and Congo red in aqueous solution was analyzed by UV analysis (UV-2450 spectrophotometer, Japan) at the wavelength of 381.1, 463.5 and 498.0 nm, respectively.

2.4. Adsorption of p-nitroaniline, methyl orange and Congo red onto HJ-C01 resin from aqueous solution

About 0.100 g of the resin was accurately weighed and 50 ml of the adsorbate aqueous solution with known concentration C_0 (mg/L) were added into a cone-shaped flask, the initial concentrations of the adsorbate were set to be about 100–500 mg/L with 100 mg/L interval. The flasks were then shaken in a thermostatic oscillator with an invariable speed (150 rmp) at 303 K for about 24 h so that the adsorption reaches equilibrium. The equilibrium concentration of the adsorbate C_e (mg/L) was analyzed and the equilibrium adsorption capacity onto the resin q_e (mg/g) was calculated by conducting a mass balance before and after the experiment as:

$$q_e = \frac{(C_0 - C_e)V}{W} \quad (2)$$

where V was the volume of the solution (L) and W was the mass of the resin (g).

2.5. Fixed-bed column experiment

The fixed-bed column experiment was carried out by a glass column (16 mm diameter and 290 mm length) at room temperature and 10 ml of wet resin was packed in the glass column. A HL-2 pump (Shanghai Huxi Analysis Instrument Factory Co. Ltd., China) was used to ensure a constant flow rate. 2.0 mmol/L of the adsorbate solution were passed through the column at a flow rate of 6 BV/h (1 BV = 10 ml), and concentration of the adsorbate from the effluent were recorded until concentration of adsorbate from the effluent was almost equal to the initial one.

3. Results and discussion

3.1. Characterization of the resin

3.1.1. Pore structure of HJ-C01 resin

As listed in Table 2, the BET specific surface area and pore volume of HJ-C01 are much higher than those of macroporous cross-linked PS [14,16]. Moreover, the average pore diameter of HJ-C01 is 2.39 nm, indicative of its microporous structure. The results of elemental analysis indicate that oxygen element is also existent except for carbon, hydrogen and chlorine elements, and the oxygen content is up to 3.3%, which may be from oxidation of chloromethyl groups of gel-type chloromethylated PS in Friedel–Crafts reaction [20].

Fig. 2(a) shows the N_2 adsorption–desorption isotherm of HJ-C01, it is seen that the adsorption isotherm is a typical Langmuir adsorption isotherm and it seems very close to type-I isotherm, suggesting that HJ-C01 possesses narrow pore diameter distribution and predominant microporous/mesoporous structure. At the initial part of the adsorption isotherm with a relative pressure below 0.05, the N_2 adsorption capacity increases rapidly with increment of the relative pressure, proving that micropores even super-micropores are existent. Then N_2 adsorption capacity gradually increases with increasing of the relative pressure till adsorption equilibrium is reached. The visible hysteresis loop of the desorption isotherm indicates that mesopores are also present. Fig. 2(b) and (c) displays the pore diameter distribution of HJ-C01 by incremental specific surface area and pore volume, and it is obvious that micropores/mesopores give a main contribution to the whole BET specific surface area and pore volume. The scanning electron microscope (SEM) photo of HJ-C01 is shown in Fig. 1(d).

3.1.2. Surface chemical structure of HJ-C01 resin

FT-IR spectrum is a useful tool to identify some specific functional groups on the resin because a specific chemical bond has a unique vibrational band in the FT-IR spectrum. As displayed in Fig. 2(e), after Friedel–Crafts reaction, most of the vibrations remain unchanged except that two strong vibrational bands related to CH_2Cl groups at 1265 and 669 cm^{-1} are greatly weakened, and another moderate C=O stretching band involved in formaldehyde carbonyl groups appears with frequency at 1704 cm^{-1}, and this may be from oxidation of the CH_2Cl groups of chloromethylated PS [20].

3.2. Adsorption isotherms from the single adsorbate solution

Fig. 3 depicts the adsorption isotherms of *p*-nitroaniline, methyl orange and Congo red onto HJ-C01 from the single adsorbate (*p*-nitroaniline or methyl orange or Congo red) solution. It is seen that the adsorption of *p*-nitroaniline onto HJ-C01 is very effective and the equilibrium adsorption capacity arrives at 180.0 mg/L at the equilibrium concentration of 100 mg/L. Additionally, the temperature is not favorable for the adsorption and the adsorption capacity of *p*-nitroaniline onto HJ-C01 decreases with increasing of the temperature. Meanwhile, it can be observed that the adsorption capacity of *p*-nitroaniline is the largest among the three adsorbates and it follows an order as: $q_{e(p\text{-nitroaniline})} > q_{e(\text{methyl orange})} > q_{e(\text{Congo red})}$, and nearly no Congo red is adsorbed on HJ-C01. The molecular sizes of *p*-nitroaniline, methyl orange and Congo red are predicted to be 0.67 nm × 0.43 nm, 1.19 nm × 0.68 nm × 0.37 nm and 2.29 nm × 0.82 nm × 0.60 nm, respectively (Table 1), which has an order as: *p*-nitroaniline < methyl orange < Congo red. That is, the larger the molecular size of the adsorbate is, the smaller the adsorption capacity of the adsorbate on the resin is, indicative of molecular sieving effect of HJ-C01. The average pore diameter of HJ-C01 is 2.39 nm, almost equal to the molecular size of Congo red, inducing no adsorption capacity on HJ-C01.

The BET specific surface area of the adsorbent, the polarity matching between the adsorbent and the adsorbate, pore structure of the adsorbent and the matching of the pore size of the adsorbent with the size of the adsorbate are thought to be the main factors influencing the adsorption. The BET specific surface area of HJ-C01 is very high (1546.9 m^2/g) and the micropore specific surface area of HJ-C01 is especially dominant, favoring the adsorbate–adsorbate interaction. The surface on HJ-C01 is modified with a few polar formaldehyde carbonyl groups, *p*-nitroaniline is also a polar molecule, and the polarity matching between HJ-C01 and *p*-nitroaniline enhances the surface adsorption. The micropores/

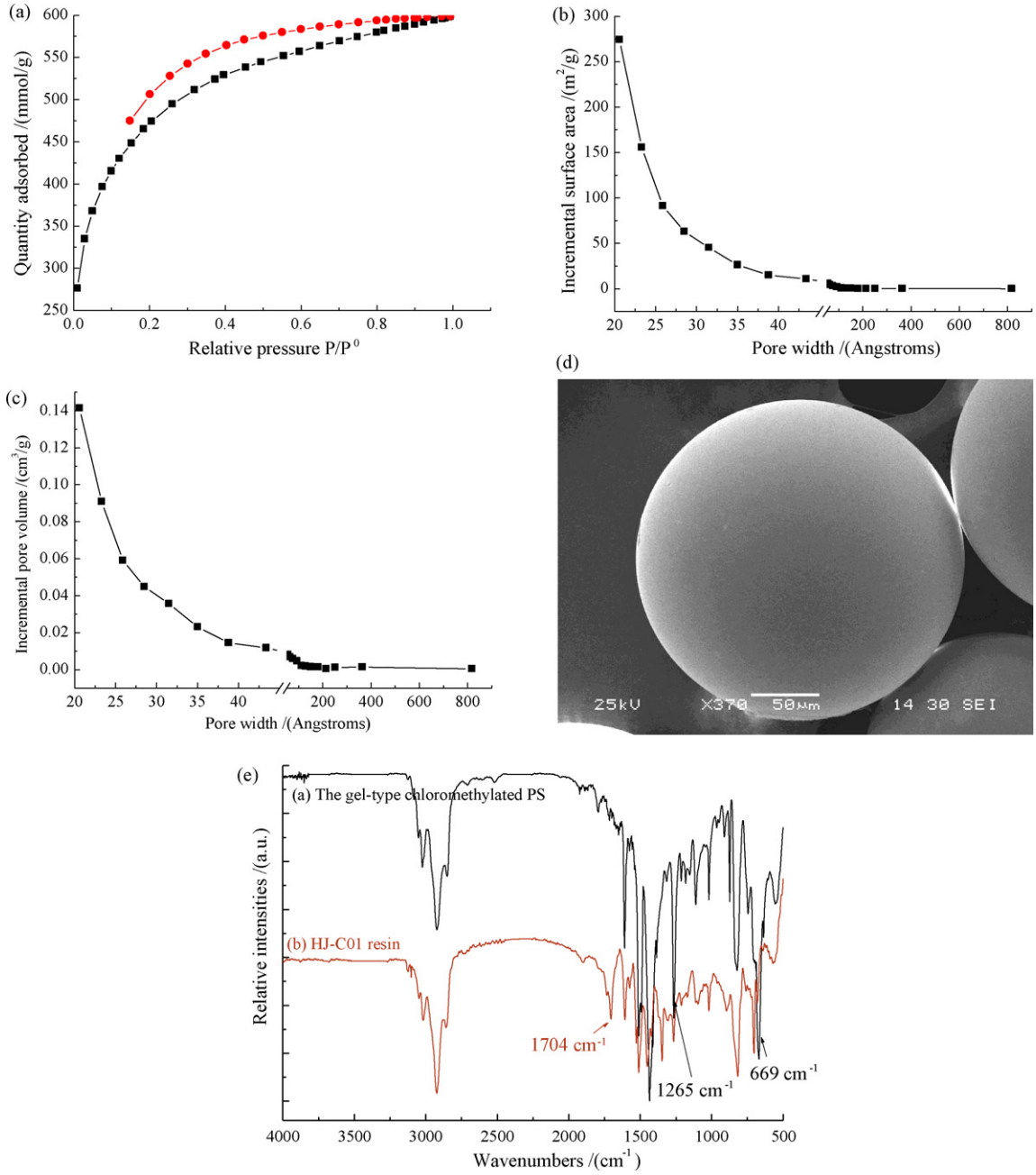

Fig. 2. Characterization of HJ-C01 resin. (a) N_2 adsorption–desorption isotherms; (b) pore diameter distribution with regard to the incremental specific surface area; (c) pore diameter distribution for the incremental pore volume; (d) scanning electron microscope (SEM) photo; (e) FT-IR spectra.

mesopores play a predominant role in the pore structure for HJ-01 resin, which is suitable for the adsorbate–adsorbate interaction via pore filling mechanism. The average pore diameter of HJ-C01 is about 3.6 times greater than the molecular size of *p*-nitroaniline, falling in the optimum ratio of the pore diameter of the adsorbent to the molecular size of the adsorbate, which is suitable for the adsorption. Therefore, the high BET specific surface area especially the micropore specific surface area, the polar formaldehyde carbonyl groups, predominant microporous/mesoporous structure and the matching of the pore diameter of HJ-C01 with the molecular size of *p*-nitroaniline are the possible reasons for the excellent adsorption efficiency for *p*-nitroaniline adsorbed on HJ-C01.

Langmuir and Freundlich isotherm models are adopted to describe the adsorption isotherm data [21,22], the regression equations, the parameters K_L, K_F, n and correlation coefficients R^2 fitted by Langmuir and Freundlich isotherms are summarized in Table 3. It is observed that Freundlich isotherm model characterizes the adsorption equilibrium data better than Langmuir one due to $R^2 > 0.99$, suggesting that the adsorption is a multi-layer adsorption process.

3.3. Adsorption isotherms from the mixed adsorbate solution

If the adsorption isotherms in Fig. 3 are fitted by linear fitting method, the slopes of the three fitted adsorption isotherms follow an order as: $k_{p\text{-nitroaniline}} > k_{\text{methyl orange}} > k_{\text{Congo red}}$, and the ratio of $k_{p\text{-nitroaniline}}$ to $k_{\text{methyl orange}}$ as well as that of $k_{p\text{-nitroaniline}}$ to $k_{\text{Congo red}}$ can be calculated to be 7.06 and 41.40, respectively, implying that HJ-C01 can separate *p*-nitroaniline from methyl orange (or Congo red) effectively. Therefore, the adsorption from the mixed

Table 3
The fitted results for the adsorption of *p*-nitroaniline, methyl orange and Congo red onto HJ-C01 resin according to Langmuir and Freundlich isotherm models.

Langmuir isotherm model	Regression equations	q_m (mg/g)	K_L (L/mg)	R^2
p-Nitroaniline	$C_e/q_e = 0.003780C_e + 0.1314$	264.5	0.02877	0.9892
Methyl orange	$C_e/q_e = 0.008460C_e + 0.3218$	118.2	0.02629	0.9861
Congo red	$C_e/q_e = -0.04680C_e + 44.73$	–	–	0.9068
Freundlich isotherm model	**Regression equations**	K_F [(mg/g)(L/mg)$^{1/n}$]	n	R^2
p-Nitroaniline	$\log q_e = 1.238 + 0.5472 \log C_e$	17.30	1.828	0.9927
Methyl orange	$\log q_e = 1.285 + 0.3057 \log C_e$	19.26	3.271	0.9935
Congo red	$\log q_e = -2.323 + 1.348 \log C_e$	0.0048	0.7418	0.9999

adsorbate (*p*-nitroaniline/methyl orange or *p*-nitroaniline/Congo red) solution is performed, and the results are displayed in Fig. 4(a) and (b). Comparing the adsorption isotherm of *p*-nitroaniline from the single adsorbate solution with the corresponding one from the mixed adsorbate solution, it can be concluded that the adsorption of *p*-nitroaniline is slightly weakened from the mixed adsorbate solution, whereas the adsorption of methyl orange (or Congo red) remains equivalent, which indicates that methyl orange or Congo red can influence the adsorption of *p*-nitroaniline.

The adsorption isotherm data in Fig. 4 are also fitted by Langmuir and Freundlich isotherm models (Table 4(a) and (b)). It is shown that Freundlich isotherm can characterize the adsorption isotherms better than Langmuir ones. Comparing the values of K_F and n of *p*-nitroaniline from the mixed adsorbate solution with those from the single adsorbate solution, it is seen that the values of K_F and n from *p*-nitroaniline and methyl orange solution are greater than those from the single solution, while those from *p*-nitroaniline and Congo red solution is less than those from the single solution, revealing that the effect of methyl orange on the adsorption of *p*-nitroaniline is different from that of Congo red.

3.4. *Effect of methyl orange and Congo red on the adsorption of p-nitroaniline*

The effect of methyl orange as well as that of Congo red on the adsorption of *p*-nitroaniline onto HJ-C01 is investigated subsequently and the results are illustrated in Fig. 5(a) and (b). It is shown that low concentration of methyl orange (<200 mg/L) has a positive effect on the adsorption of *p*-nitroaniline, whereas high concentration of methyl orange (>200 mg/L) poses a negative effect. The reasons may be from the fact as follows. Methyl orange is more water-soluble than *p*-nitroaniline in aqueous solution (the solubility of methyl orange and *p*-nitroaniline are about 0.01 g/100 mL H_2O and 0.0008 g/100 mL H_2O, respectively [23]). As a small quantity of methyl orange is added into the *p*-nitroaniline solution, many water molecules are captured to dissolve methyl orange, which results in a "salt-out" effect for *p*-nitroaniline [24], inducing an enhanced adsorption of *p*-nitroaniline. As the concentration of methyl orange is considerably high, the competitive adsorption of methyl orange onto HJ-C01 cannot be ignored, resulting in a weakened adsorption of *p*-nitroaniline. As far as Congo red is concerned, it is clear that Congo red affects the adsorption of *p*-nitroaniline in a negative way, which may be from the reason that Congo red can

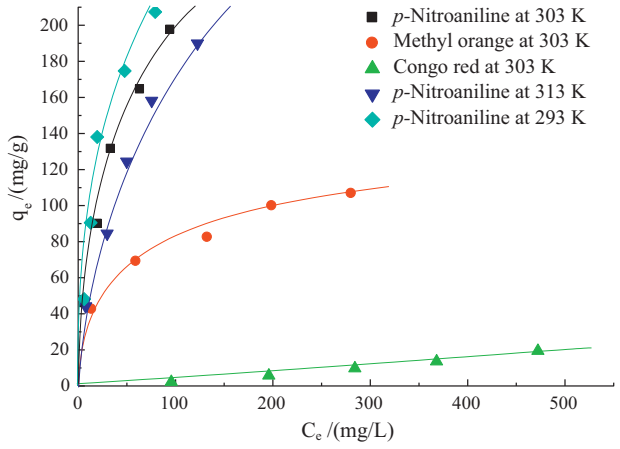

Fig. 3. The adsorption isotherms of *p*-nitroaniline, methyl orange and Congo red onto HJ-C01 resin from the single adsorbate solution (about 0.100 g of HJ-C01 resin, 50 ml of the adsorbate aqueous solution, the initial concentrations of the adsorbate were set to be about 100, 200, 300, 400 and 500 mg/L, the agitation speed of the thermostatic oscillator was 150 rmp, adsorption time: about 24 h).

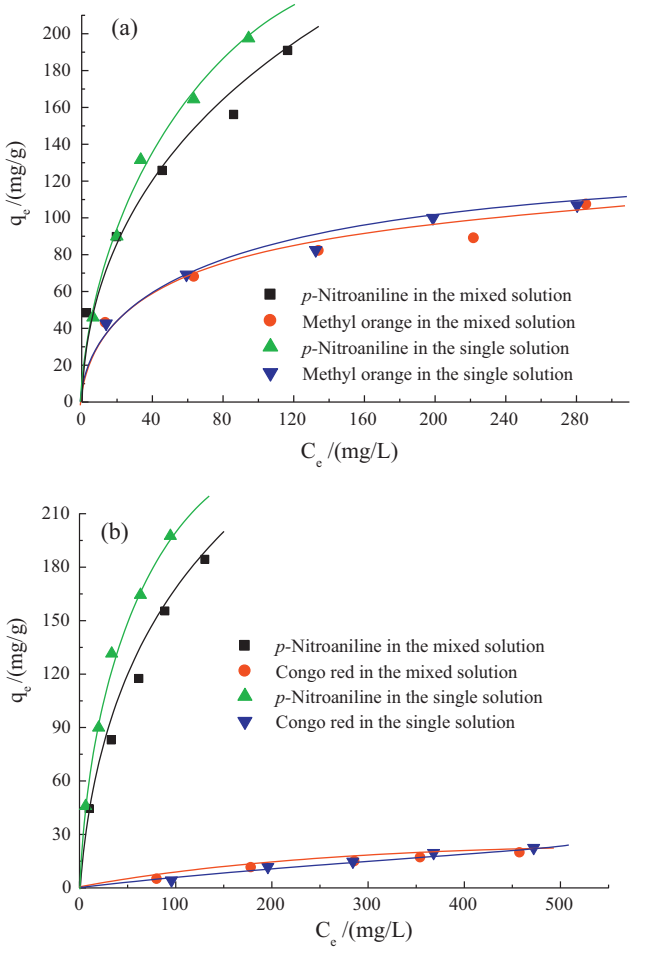

Fig. 4. The adsorption isotherms onto HJ-C01 resin at 303 K from the mixed adsorbate solution. (a) *p*-Nitroaniline and methyl orange; (b) *p*-nitroaniline and Congo red (about 0.100 g of HJ-C01 resin, 50 ml of the adsorbate aqueous solution, the initial concentrations of the respective adsorbate: 100, 200, 300, 400 and 500 mg/L, the agitation speed of the thermostatic oscillator: 150 rmp, adsorption time: about 24 h, T = 303 K).

Table 4
(a) The fitted results for the adsorption of *p*-nitroaniline (or methyl orange) onto HJ-C01 resin at 303 K with the mixed adsorbate (*p*-nitroaniline and methyl orange) solution according to Langmuir and Freundlich isotherm models. (b) The fitted results for the adsorption of *p*-nitroaniline (or Congo red) onto HJ-C01 resin at 303 K with the mixed adsorbate (*p*-nitroaniline and Congo red) solution according to Langmuir and Freundlich isotherm models.

Langmuir model	Regression equations	q_m (mg/g)	K_L (L/mg)	R^2
(a)				
p-Nitroaniline	$C_e/q_e = 0.004760C_e + 0.1039$	210.1	0.04581	0.9551
Methyl orange	$C_e/q_e = 0.008870C_e + 0.3335$	112.7	0.02661	0.9721
Freundlich model	**Regression equations**	K_F [(mg/g)(L/mg)$^{1/n}$]	n	R^2
(a)				
p-Nitroaniline	$\log q_e = 1.501+0.3639 \log C_e$	31.67	2.748	0.9929
Methyl orange	$\log q_e = 1.316+0.2820 \log C_e$	20.68	3.546	0.9905
Langmuir model	**Regression equation**	q_m (mg/g)	K_L (L/mg)	R^2
(b)				
p-nitroaniline	$C_e/q_e = 0.003700C_e + 0.2504$	270.3	0.01480	0.9488
Congo red	$C_e/q_e = 0.02000C_e + 13.69$	50.00	0.001460	0.8996
Freundlich model	**Regression equation**	K_F [(mg/g)(L/mg)$^{1/n}$]	n	R^2
(b)				
p-Nitroaniline	$\log q_e = 1.052 + 0.5741 \log C_e$	11.28	1.742	0.9973
Congo red	$\log q_e = -0.7959 + 0.7966 \log C_e$	0.1600	1.255	0.9936

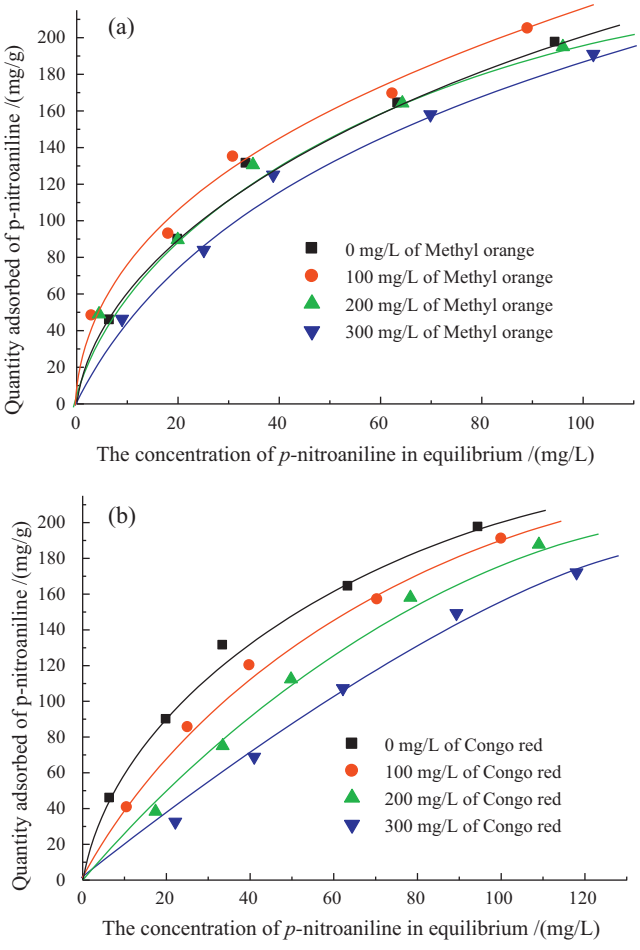

Fig. 5. The effect of (a) methyl orange and (b) Congo red on the adsorption of *p*-nitroaniline onto HJ-C01 resin from aqueous solution with the temperature at 303 K (about 0.100 g of HJ-C01 resin, 50 ml of the *p*-nitroaniline aqueous solution, the initial concentrations of *p*-nitroaniline: 100, 200, 300, 400 and 500 mg/L, the agitation speed of the thermostatic oscillator: 150 rmp, concentration of methyl orange or Congo red in the solution: 0, 100, 200 and 300 mg/L, adsorption time: about 24 h, T = 303 K).

block the pores of HJ-C01, which prevents *p*-nitroaniline molecules from diffusing into the pore of HJ-C01.

The adsorption isotherm data in Fig. 5 are also fitted by Freundlich isotherm models (Table 5). It is obvious that the values of K_F and n firstly increase and then decrease with increasing of the concentration of methyl orange, which further confirms that the positive effect at a low concentration and then the negative effect at a high concentration of methyl orange on the adsorption of *p*-nitroaniline. With regard to Congo red, the values of K_F and n decrease with increment of the concentration of Congo red, proving the negative effect of Congo red on the adsorption.

3.5. Dynamic adsorption and separation of *p*-nitroaniline from the mixed adsorbate solution

HJ-C01 resin possesses excellent adsorption efficiency for *p*-nitroaniline, it may also separate *p*-nitroaniline from methyl orange or Congo red from the mixed adsorbate solution. It is hopeful that this resin can be developed as a polymeric adsorbent for adsorptive removal of *p*-nitroaniline from wastewater and it is also hopeful that this resin can be applied as the adsorbent to separate *p*-nitroaniline from other molecules with a larger molecular size like methyl orange and Congo red. Therefore, it is necessary to test its dynamic adsorption property.

Fig. 6 displays the result of mini-column dynamic adsorption *p*-nitroaniline from the single adsorbate solution, those of *p*-nitroaniline, methyl orange and Congo red from the mixed adsorbate solution are also shown in Fig. 6, where C_0 is the initial concentration (mg/L), and C_v is the concentration at different bed volume of the effluent (mg/L). The breakthrough points of *p*-nitroaniline from the single adsorbate solution is measured to be 93 BV, whereas the breakthrough points of *p*-nitroaniline and methyl orange from the mixed solution are measured to be 85 and 38 BV, respectively. That is, HJ-C01 can separate methyl orange from *p*-nitroaniline as the effluent is in the range of 38–85 BV. Congo red cannot be adsorbed on HJ-C01 and it is leaked out directly, implying that HJ-C01 can separate *p*-nitroaniline from Congo red completely. As the HJ-C01 column which has adsorbed *p*-nitroaniline and methyl orange (or Congo red) is subjected to 1% of hydrochloric acid aqueous solution, nearly 100% regeneration efficiency is achieved. Continuous adsorption-regeneration run of the used HJ-C01 bed is performed and the fifth cycle is seen

Table 5
The fitted results for the adsorption of *p*-nitroaniline with different concentration of methyl orange or Congo red at 303 K according to Freundlich isotherm model.

	Regression equation	K_F [(mg/g)(L/mg)$^{1/n}$]	n	R^2
Concentration of methyl orange				
0 mg/L	$\log q_e = 1.238 + 0.5472 \log C_e$	17.30	1.828	0.9927
100 mg/L	$\log q_e = 1.474 + 0.4246 \log C_e$	29.76	2.355	0.9901
200 mg/L	$\log q_e = 1.390 + 0.4554 \log C_e$	24.54	2.196	0.9934
300 mg/L	$\log q_e = 1.113 + 0.5905 \log C_e$	12.98	1.694	0.9886
Concentration of Congo red				
0 mg/L	$\log q_e = 1.238 + 0.5472 \log C_e$	17.30	1.828	0.9927
100 mg/L	$\log q_e = 0.9478 + 0.6810 \log C_e$	8.867	1.486	0.9823
200 mg/L	$\log q_e = 0.5234 + 0.8776 \log C_e$	3.337	1.140	0.9867
300 mg/L	$\log q_e = 0.1817 + 1.012 \log C_e$	1.520	0.9878	0.9860

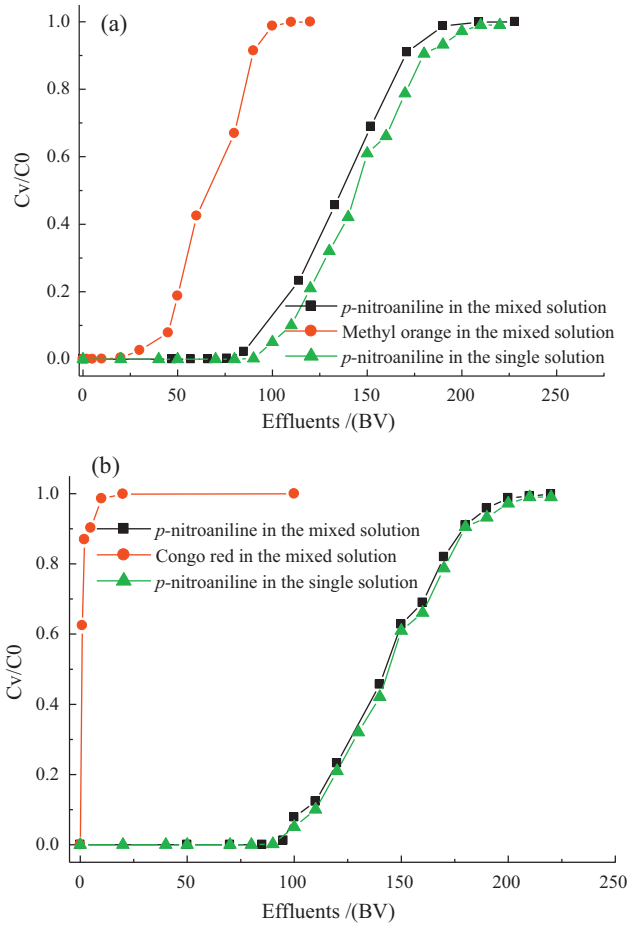

Fig. 6. The dynamic adsorption onto HJ-C01 resin. (a) *p*-Nitroaniline and methyl orange; (b) *p*-nitroaniline and Congo red (the concentration of *p*-nitroaniline, methyl orange and Congo red was set to be 2.0 mmol/L, the flow rate was set to be 6 BV/h, room temperature).

almost identical to the first cycle (not displayed), implying that HJ-C01 can be completely regenerated and its adsorption efficiency is excellent.

4. Conclusions

A novel hyper-cross-linked polymeric adsorbent HJ-C01 was prepared successfully from gel-type chloromethylated PS by Friedel–Crafts reaction and it possessed high BET specific surface area, microporous/mesoporous structure and a few formaldehyde carbonyl groups on its surface. It could adsorb *p*-nitroaniline from aqueous solution effectively and it can separate *p*-nitroaniline from methyl orange and Congo red from aqueous solution, indicating a molecular sieving effect.

Acknowledgments

The financial support from the National Natural Science Foundation of China (No. 20804058) and the Science and Technology Project of Changsha city (No. k1003036-31) were greatly acknowledged.

References

[1] A. Aranda, J.M. López, R. Murillo, A.M. Mastral, A. Dejoz, I. Vázquez, B. Solsona, S.H. Taylor, T. García, Total oxidation of naphthalene with high selectivity using a ceria catalyst prepared by a combustion method employing ethylene glycol, J. Hazard. Mater. 171 (2009) 393–399.
[2] Y. Ran, K. Sun, X. Ma, G. Wang, P. Grathwohl, E.Y. Zeng, Effect of condensed organic matter on solvent extraction and aqueous leaching of polycyclic aromatic hydrocarbons in soils and sediments, Environ. Pollut. 148 (2007) 529–538.
[3] M. Shamsipur, J. Hassan, A novel miniaturized homogeneous liquid–liquid solvent extraction-high performance liquid chromatographic-fluorescence method for determination of ultra traces of polycyclic aromatic hydrocarbons in sediment samples, J. Chromatogr. A 1217 (2010) 4877–4882.
[4] T. Garcia, B. Solsona, D. Cazorla-Amorós, Á. Linares-Solano, S.H. Taylor, Total oxidation of volatile organic compounds by vanadium promoted palladium-titania catalysts: comparison of aromatic and polyaromatic compounds, Appl. Catal. B 62 (2006) 66–76.
[5] X.W. Zeng, Y.G. Fan, G.L. Wu, C.H. Wang, R.F. Shi, Enhanced adsorption of phenol from water by a novel polar post-crosslinked polymeric adsorbent, J. Hazard. Mater. 169 (2009) 1022–1028.
[6] E. Ayranci, O. Duman, Adsorption of aromatic organic acids onto high area activated carbon cloth in relation to wastewater purification, J. Hazard. Mater. 136 (2006) 542–552.
[7] S.H. Lin, R.S. Juang, Adsorption of phenol and its derivatives from water using synthetic resins and low-cost natural adsorbents: a review, J. Environ. Manag. 90 (2009) 1336–1349.
[8] X.W. Zeng, T.J. Yu, P. Wang, R.H. Yuan, Q. Wen, Y.G. Fan, C.H. Wang, R.F. Shi, Preparation and characterization of polar polymeric adsorbents with high surface area for the removal of phenol from water, J. Hazard. Mater. 177 (2010) 773–780.
[9] F.C. Wu, R.L. Tseng, R.S. Juang, Initial behavior of intraparticle diffusion model used in the description of adsorption kinetics, Chem. Eng. J. 153 (2009) 1–8.
[10] M.P. Tsyurupa, L.A. Maslova, A.I. Andreeva, T.A. Mrachkovskaya, V.A. Davankov, Sorption of organic compounds from aqueous media by hypercrosslinked polystyrene sorbents "Styrosorb", React. Polym. 25 (1995) 69–78.
[11] V.A. Davankov, C.S. Sychov, M.M. Ilyin, K.O. Sochilina, Hypercrosslinked polystyrene as a novel type of high-performance liquid chromatography column packing material: mechanisms of retention, J. Chromatogr. A 987 (2003) 67–75.
[12] V.V. Podlesnyuk, J. Hradil, E. Králová, Sorption of organic vapors by macroporous and hypercrosslinked polymeric adsorbents, React. Funct. Polym. 42 (1999) 181–191.
[13] V.V. Azanova, J. Hradil, Sorption properties of macroporous and hypercrosslinked copolymers, React. Funct. Polym. 41 (1999) 163–175.
[14] J.H. Ahn, J.E. Jang, C.G. Oh, S.K. Ihm, J. Cortez, D.C. Sherrington, Rapid generation and control of microporosity, bimodal pore size distribution, and surface area in Davankov-type hyper-cross-linked resins, Macromolecules 39 (2006) 627–632.
[15] Z Wang, R.B. Bai, Y.P. Ting, Conversion of waste polystyrene into porous and functionalized adsorbent and its application in humic acid removal, Ind. Eng. Chem. Res. 47 (2008) 1861–1867.
[16] F.S. Macintyre, D.C. Sherrington, Control of porous morphology in suspension polymerized poly(divinylbenzene) resins using oligomeric porogens, Macromolecules 37 (2004) 7628–7636.

[17] M.D. Jia, K.V. Peinemann, R.D. Behling, Molecular sieving effect of the zeolite-filled silicone rubber membranes in gas permeation, J. Membr. Sci. 57 (1991) 289–296.
[18] M.J. Frisch, G.W. Trucks, H.B. Schlegel, G.E. Scuseria, M.A. Robb, J.R. Cheeseman, J.A. Montgomery Jr., T. Vreven, K.N. Kudin, J.C. Burant, J.M. Millam, S.S. Iyengar, J. Tomasi, V. Barone, B. Mennucci, M. Cossi, G. Scalmani, N. Rega, G.A. Petersson, H. Nakatsuji, M. Hada, M. Ehara, K. Toyota, R. Fukuda, J. Hasegawa, M. Ishida, T. Nakajima, Y. Honda, O. Kitao, H. Nakai, M. Klene, X. Li, J.E. Knox, H.P. Hratchian, J.B. Cross, C. Adamo, J. Jaramillo, R. Gomperts, R.E. Stratmann, O. Yazyev, A.J. Austin, R. Cammi, C. Pomelli, J.W. Ochterski, P.Y. Ayala, K. Morokuma, G.A. Voth, P. Salvador, J.J. Dannenberg, V.G. Zakrzewski, S. Dapprich, A.D. Daniels, M.C. Strain, O. Farkas, D.K. Malick, A.D. Rabuck, K. Raghavachari, J.B. Foresman, J.V. Ortiz, Q. Cui, A.G. Baboul, S. Clifford, J. Cioslowski, B.B. Stefanov, G. Liu, A. Liashenko, P. Piskorz, I. Komaromi, R.L. Martin, D.J. Fox, T. Keith, M.A. Al-Laham, C.Y. Peng, A. Nanayakkara, M. Challacombe, P.M.W. Gill, B. Johnson, W. Chen, M.W. Wong, C. Gonzalez, J.A. Pople, GAUSSIAN 03, Revision B.05, Gaussian, Inc., Pittsburgh, PA, 2003.
[19] C.P. Wu, C.H. Zhou, F.X. Li, Experiments of Polymeric Chemistry, first ed., Anhui Science and Technology Press, Hefei, 1987.
[20] G.H. Meng, A.M. Li, W.B. Yang, F.Q. Liu, X. Yang, Q.X. Zhang, Mechanism of oxidative reaction in the post crosslinking of hyper-crosslinked polymers, Eur. Polym. J. 43 (2007) 2732–2737.
[21] A.M. Li, Q.X. Zhang, G.C. Zhang, J.L. Chen, Z.H. Fei, F.Q. Liu, Adsorption of phenolic compounds from aqueous solutions by a water-compatible hypercrosslinked polymeric adsorbent, Chemosphere 47 (2002) 981–989.
[22] A.J. Glemza, K.L. Mardis, A.A. Chaudhry, M.K. Gilson, G.F. Payne, Competition between intra- and intermolecular hydrogen bonding: effect on para/ortho adsorptive selectivity for substituted phenols, Ind. Eng. Chem. Res. 39 (2000) 463–472.
[23] J.T. Wang, Q.M. Hu, B.S. Zhang, Y.M. Wang, Organic Chemistry, second ed., Nankai University Press, Tianjing, 1998.
[24] M. Chorro, N. Kamenka, B. Faucompre, S. Partyka, M. Lindheimer, R. Zana, Micellization and adsorption of a zwitterionic surfactant: N-dodecyl betaine-effect of salt, Colloids Surf. A 110 (1996) 249–261.